JPn Neuroscience

The Journal of Physiology

J Physiol 592.13 (2014) pp 2829–2844

Balance between the proximal dendritic compartment and the soma determines spontaneous firing rate in midbrain dopamine neurons

Jinyoung Jang[1,2], Ki Bum Um[1], Miae Jang[1], Shin Hye Kim[2], Hana Cho[1,2], Sungkwon Chung[1,2], Hyun Jin Kim[1,2] and Myoung Kyu Park[1,2]

[1] *Department of Physiology, Sungkyunkwan University School of Medicine, 300 Chunchun-dong, Jangan-ku, Suwon, 440-746, Korea*
[2] *Center For Molecular Medicine, Samsung Biomedical Research Institute, 300 Chunchun-dong, Jangan-ku, Suwon, 440-746, Korea*

Key points

- The electrical coupling between the soma and dendritic compartments has been regarded as a key determinant for the spontaneous firing rate (SFR) in midbrain dopamine neurons.
- Isolated nigral dopamine neurons showed a wide range of soma size and a variable number of primary dendrites but preserved a quite consistent SFR.
- The SFR was not correlated with soma size or with the number of primary dendrites, but it was strongly correlated with the area ratios of the proximal dendritic compartments to the somatic compartment.
- Tetrodotoxin puff and local Ca^{2+} perturbation experiments, computer simulation, and local glutamate uncaging experiments suggest the importance of the proximal dendritic compartments in pacemaker activity.
- These results lead us to a novel conclusion that the proximal dendritic compartments, not the whole dendritic compartments, play a key role in the somatodendritic balance that determines the SFR in dopamine neurons.

Abstract Midbrain dopamine (DA) neurons are slow intrinsic pacemakers that require the elaborate composition of many ion channels in the somatodendritic compartments. Understanding the major determinants of the spontaneous firing rate (SFR) of midbrain DA neurons is important because they determine the basal DA levels in target areas, including the striatum. As spontaneous firing occurs synchronously at the soma and dendrites, the electrical coupling between the soma and dendritic compartments has been regarded as a key determinant for the SFR. However, it is not known whether this somatodendritic coupling is served by the whole dendritic compartments or only parts of them. In the rat substantia nigra pars compacta (SNc) DA neurons, we demonstrate that the balance between the proximal dendritic compartment and the soma determines the SFR. Isolated SNc DA neurons showed a wide range of soma size and a variable number of primary dendrites but preserved a quite consistent SFR. The SFR was not correlated with soma size or with the number of primary dendrites, but it was strongly correlated with the area ratios of the proximal dendritic compartments to the somatic compartment. Tetrodotoxin puff and local Ca^{2+} perturbation experiments, computer simulation, and local glutamate uncaging experiments suggest the importance of the proximal dendritic compartments in pacemaker activity. These data indicate that the proximal dendritic compartments, not the whole dendritic compartments, play a key role in the somatodendritic balance that determines the SFR in DA neurons.

DOI: 10.1113/jphysiol.2014.275032

(Resubmitted 26 March 2014; accepted after revision 17 April 2014; first published online 22 April 2014)
Corresponding authors M. K. Park: Department of Physiology, Sungkyunkwan University School of Medicine, 300 Chunchun-dong, Jangan-ku Suwon 440–746, Korea. Email: mkpark@skku.edu; H. J. Kim: Email: kimhyunjin@skku.edu

Abbreviations ANOVA, analysis of variance; AP, action potential; CV, coefficient of variation; DA, dopamine; MNI-glutamate, 4-methoxy-7-nitroindolinyl-caged L-glutamate; NP-EGTA, *o*-nitrophenyl EGTA; SD, Sprague Dawley; SEM, standard error of the mean; SFR, spontaneous firing rate; SK, skewness coefficient; SK channel, small conductance calcium-activated potassium channel; SNc, substantia nigra pars compacta; SOP, slow oscillatory potential; TH, tyrosine hydroxylase; TTX, tetrodotoxin.

Introduction

Intrinsic excitability of ion channels residing in the midbrain dopamine (DA) neurons generates autonomous and regular action potentials (APs) at 2–5 Hz (Grace & Bunney, 1983*a*,*b*), which are essential for maintaining ambient DA levels and the DA signalling necessary for normal functioning of basal ganglia, such as the striatum (Ball, 2001; Morikawa & Paladini, 2011; Surmeier *et al.* 2012). Many ion channels have been suggested to play a critical role in this autonomous firing with remarkable conflicts; while a possible pacemaking role of $Ca_v1.3$ channels is highly controversial (Nedergaard *et al.* 1993; Mercuri *et al.* 1994; Kim *et al.* 2007; Puopolo *et al.* 2007; Guzman *et al.* 2009; Putzier *et al.* 2009), other channels, such as Na_v ion channels, hyperpolarization/cyclic nucleotide-gated channels and non-selective cation channels, appear to be involved in pacemaking activity (Kim *et al.* 2007; Guzman *et al.* 2009; Kuznetsova *et al.* 2010; Tucker *et al.* 2012). In addition to the ion channels, pacemaker activity in neurons is critically affected by morphological features. It is well known that the midbrain DA neurons extend multiple excitable dendrites and that an axon originates from one of them (Hausser *et al.* 1995; Gentet & Williams, 2007). As both APs and Ca^{2+} transients measured at dendrites during a pacemaking cycle are synchronized with those in the soma (Wilson & Callaway, 2000; Guzman *et al.* 2009), it has been assumed that the soma is electrically coupled with dendritic compartments and that the whole somatodendritic compartment participates in pacemaking. Therefore, most present simulation experiments assume a homogeneous distribution of most ion channels throughout the whole somatodendritic compartment with a few exceptions, such as A-type K^+ channels and Na_v channels (Kuznetsova *et al.* 2010; Drion *et al.* 2011; Tucker *et al.* 2012). Therefore, dendritic excitability seems to be crucial in the generation and modulation of pacemaker activities in DA neurons (Kuznetsov *et al.* 2006, 2010). Consequently, there are many simulation models based on the different amounts of ion channels engaged in the soma and dendritic compartments (Wilson & Callaway, 2000; Kuznetsova *et al.* 2010; Drion *et al.* 2011; Tucker *et al.* 2012). But surprisingly, although many simulation experiments suggest that distribution of ion channels in the somatodendritic compartments and dendritic architectures are critical factors for determining the spontaneous firing rate (SFR) (Kuznetsova *et al.* 2010; Drion *et al.* 2011; Tucker *et al.* 2012), little is known about the morphological features and dendritic properties of real, individual DA neurons that determine the SFR. One important step in understanding the pacemaking mechanism may be to establish a functional, geometrical model for pacemaking in this highly polarized neuron. But it is still not known whether the entire dendritic compartments or parts of dendrites contribute to pacemaking and/or determination of the SFR in real DA neurons. Here, by taking advantage of acutely isolated DA neurons that preserve regular spontaneous firing activities and a substantial amount of multiple dendrites (Choi *et al.* 2006; Jang *et al.* 2011*a*; Kim *et al.* 2013), we show that the proximal dendritic compartments, not the whole dendritic compartments, play a key role in the somatodendritic balance determining SFR in midbrain DA neurons.

Methods

Neuron preparation

All experiments were conducted according to the Sungkyunkwan University School of Medicine Animal Care and Use Committee's approved protocols. Sprague Dawley (SD) rats were anaesthetized with isofluane and decapitated. One hundred and thirty male and female rats were used. Single DA neurons were acutely dissociated from postnatal days 9–12 SD rats. The solution for neuron dissociation was fully oxygenated by 100% O_2. The brain was rapidly removed under an ice-cold high-glucose solution consisting of the following (in mM): 135 NaCl, 5 KCl, 10 Hepes, 1 $CaCl_2$, 1 $MgCl_2$ and 25 D-glucose. The solution pH was adjusted to 7.3 with NaOH. The midbrain was a coronal slice of 400 μm thickness sliced by a vibratome (Series 1000, Technical Products International, St James, MB, Canada). The substantia nigra pars compacta (SNc) regions were cut out from midbrain slices, and the DA neuron-containing tissues were then incubated in the high-glucose solution with 8 U ml^{-1} papain (Worthington Biochemical Corp., Lakewood, NJ,

USA) for 30 min at 36–37°C. After enzymatic digestion, the tissue was washed three times with 36°C high-glucose solution. Gentle serial agitation with varying pore sizes of Pasture pipettes dissociated variously shaped single neurons from the tissue. The dissociated neurons were attached on the poly-D-lysine (0.01%)-coated cover slip for 30 min at room temperature (25°C).

Immunocytochemistry

The isolated neurons were rinsed twice with phosphate-buffered saline (PBS) and fixed with 4% paraformaldehyde in PBS at 4°C for 15 min. After fixation, the neurons were washed three times for 10 min in PBS and then incubated for 10 min in permeabilization buffer (PBS containing 1% normal goat serum and 0.2% Triton X-100) at room temperature. Neurons were rinsed in PBS and blocked for 20 min in blocking buffer (PBS containing 1% normal goat serum). For tyrosine hydroxylase (TH) staining, isolated DA neurons were processed using the mouse anti-TH antibody (1:300, Abcam Inc., Cambridge, MA, USA). The neurons were incubated for 2 h in PBS-containing antibodies, goat serum and 0.2% Triton X-100 at 4°C. Then, primary antibody-loaded neurons were rinsed three times with blocking buffer and incubated with secondary antibody: Alexa 488-conjugated goat anti-mouse IgG (1:100; Invitrogen, Carlsbad, CA, USA) in blocking buffer. After incubation for 1 h at room temperature, coverslips were washed by PBS and mounted onto slides using mounting medium (Faramount aqueous mounting medium, DakoCytomation, Glostrup, Denmark). Fluorescence images were obtained using a confocal laser scanning microscope with an argon laser.

Electrophysiology

Low-resistance (2.0–3.5 MΩ) patch electrodes were pulled (MODEL PP-830, Narishige, New York, USA) from borosilicate glass capillaries of 1.5 mm outer diameter (World Precision Instruments, Sarasota, FL, USA). The patch clamp system (EPC-9, HEKA Elektronik, Lambrecht/Pfalz, Germany) was used to measure APs in isolated DA neurons. For patch clamp recording and neuron morphological analysis, we used the neuronal imaging system: Zeiss 510 confocal microscope with HeNe laser (633 nm) and a 40× oil immersion lens (numerical aperture = 1.3). We made nystatin-perforated or cell-attached patch-clamp configurations in the current-clamp mode at a sampling rate of 10 kHz filtered at 1 kHz. Patch recording pipettes were filled with the internal solution (in mM): 140 potassium gluconate, 5 KCl, 10 Hepes, 5 $MgCl_2$ and nystatin (200 μg ml^{-1}, MP Biomedicals), pH 7.2 adjusted with KOH, or a normal bath solution. The normal bath solution contained (in mM) 140 NaCl, 5 KCl, 10 Hepes, 10 D-glucose, 1 $CaCl_2$ and 1 $MgCl_2$, pH adjusted to 7.4 with NaOH.

Photolysis of caged compounds

To increase dendritic Ca^{2+} levels or to stimulate local glutamate receptors on a small area of a dendrite, we used caged compounds. To do this the bath was flooded with 10 μM *o*-nitrophenyl EGTA (NP-EGTA) (Invitrogen) or 100 μM 4-methoxy-7-nitroindolinyl-caged L-glutamate (MNI-glutamate) (Tocris Bioscience, Bristol, UK) with 10 μM glycine. Uncaging was performed using a Zeiss 510 confocal microscope equipped with a HeNe laser (633 nm), UV laser (wavelengths 351 and 364 nm) and an oil-immersion objective lens (40× with a numerical aperture of 1.3, Olympus). The HeNe laser was used for transmitted imaging during uncaging experiments. For synapse-like rapid localized stimulation, uncaging laser power and uncaging speed were set to the maximum speed and the minimum pixel time was < 1 ms.

Micropressurized injection

For the local application of tetrodotoxin (TTX) to the DA neurons to block pacemaking spikes, the Narishige microinjection system (IM 300 Microinjector) was used. The injection glass pipette was filled with the same bath solution containing 1 μM TTX, in which concentration all APs are abolished (Choi *et al.* 2003; Kim *et al.* 2007). The micropressure glass pipettes were purchased from World Precision Instruments (TW100F-4), and the pipette resistance was between 10 and 20 MΩ. The injection pressure was maintained between 275 and 345 kPa, and the single pulse duration was 0.5–1 s.

Computational models

A computer simulation of a DA neuron was performed with NEURON software, version 7.3 (http://www.neuron.yale.edu/neuron/). All parameters and files were obtained from the above website, and they were also published and established as a model neuron in a previous report by Kuznetsova *et al.* (2010). To examine how different sizes of the soma and different numbers of dendrites affect the SFR, we modified the morphology factors of the model neuron. The density and kinetics of the simulated ion channels of the model neuron were the same as the SN DA model neuron of Kuznetsova *et al.* (2010). In the simulation, we changed the soma size or dendrite numbers of the model neuron and observed the SFR after stabilization. All compartments of the model neuron were assumed to have a cylinder form. The lengths of a proximal dendrite and a distal dendrite were fixed at 50 and 150 μm, respectively. The diameter of a proximal dendrite was defined to be tapering from 2.5 to 1.5 μm, and the diameter of distal dendrite tapered from 1.5 to 0.7 μm. When we added more dendrites to the soma, we used the same parameters as for the former proximal and

distal dendritic compartments. Soma size was 840 μm^2 (length 30 μm, diameter 14 μm).

Statistics

Statistical analyses were performed with Origin 8.1 (OriginLab Corp., Northampton, MA, USA). All presented numerical values and graphical representations are given mean ± standard error of the mean (SEM), and statistical analysis was performed using one-way analysis of variance (ANOVA) tests followed by Tukey's multiple-comparison posttest ($^*P < 0.05$). In comparing characteristics of morphological factors and firing rates, we computed the coefficient of variation (CV) and the skewness coefficient (SK). Shape parameters (x-axis) were normalized by the modes of the factors, and the frequencies of each factor (y-axis) were normalized to vary between 0 and 1 (Fig. 1*G*).

Results

DA neurons in the rat SNc show morphological diversity

Dissociated DA neurons from the SNc that were confirmed by expression of TH, a marker for DA neurons, showed variable soma sizes and numbers of primary dendrites (Fig. 1*A*). Typical morphologies of dissociated DA neurons are presented in the left panel of Fig. 1*A*, in which the upper small DA neuron extends four long primary dendrites (*a*) and the lower large DA neuron shows six long primary dendrites (*b*), indicating that our dissociated DA neurons retain a substantial amount of dendrites. The diversity of soma sizes and the differing numbers of primary dendrites among the many dissociated DA neurons are depicted as shaded areas and green lines on the right area of Fig. 1*A*, respectively, with a patch pipette attached. Isolated DA neurons have a broad range of soma sizes from 360.1 to 1573.26 μm^2 ($n = 92$). The individual soma sizes of 92 DA neurons did not show a normal Gaussian distribution but instead showed a wide and right-skewed distribution (Fig. 1*B*). The soma size of the upper 20% (1114.71 ± 65.09, $n = 18$) was approximately twice that of the lower 20% (445.89 ± 8.78, $n = 18$), showing a remarkable diversity.

DA neurons are known to extend multiple primary dendrites (Kita *et al.* 1986; Grace & Onn, 1989; Stuart *et al.* 1995), and similarly, 3–6 primary dendrites were found in our isolated DA neurons (Fig. 1*A*, *D*). The DA neurons extending four dendrites existed dominantly in the rat SNc (50.5%, 48/95), and those with six dendrites were of very low percentage (2.1%, 2/95). The DA neurons attached with three or five primary dendrites occupied 32.6% (31/95) and 14.7% (14/95), respectively (Fig. 1*D*). Generally in neurons the relationship between soma size and number of dendrites seems to be variable: while the size of the soma in the propriospinal interneurons increases with an increasing number of dendrites (Saywell *et al.* 2011), the size of the soma in the α-motor neurons does not correlate with the number of dendrites (Henneman, 1957). In the isolated DA neurons, there was no correlation between the size of the soma and the number of primary dendrites (neurons with three dendrites = 630.2 ± 47.6 μm^2, neurons with four dendrites = 703.3 ± 40.8 μm^2, neurons with five dendrites = 696.4 ± 39.0 μm^2, neurons with six dendrites = 631.1 ± 113.2 μm^2, $n = 89$; Fig. 1*E*, $P = 0.79$).

Although the distributions of soma size and dendrite number did not fit the normal Gaussian distribution (Fig. 1*B*, *D*), the frequency of spontaneous firing recorded in the isolated DA neurons did show a normal Gaussian distribution (2.50 ± 0.07 Hz, Fig. 1*F*, $n = 79$ neurons). To compare distributions of the SFR with those of soma size and dendrite numbers, we made normalized distributions of these parameters using mode values (Fig. 1*G*). While the size of somata and the number of dendrites showed wide right-skewed distributions, the SFR showed a normal Gaussian distribution (Fig. 1*G*) that was narrower. Interestingly, the ratio of the proximal dendritic area (≤80 μm from the soma) to the somatic area showed a Gaussian distribution similar to that of the SFR. The differences in distributions of soma size and dendrite numbers, in contrast to the SFR distribution, could also be observed through the CV values (Fig. 1*H*) and SK (Fig. 1*I*), respectively.

Relationship between soma size or primary dendrite numbers and SFR in the model neurons and dissociated DA neurons

According to the size principle of Henneman (1957), motor units are recruited in a precise order due to the motoneuron's own physical properties; smaller motor neurons have higher membrane resistance and thus require less depolarizing current to reach the spike threshold. Therefore, soma size is the crucial factor in determining neuronal excitability and motor neuron recruitment. In DA neurons, it has been assumed that the whole membrane compartment including the soma and all the dendrites are excitable and contribute to pacemaking (Wilson & Callaway, 2000). Using a simulation model of the SNc DA neuron (Kuznetsova *et al.* 2010), we examined how soma size and differing number of primary dendrites affect SFR. While soma size is inversely related to SFR (Fig. 2*A*, *B*), the SFR was increased with increasing numbers of primary dendrites (Fig. 2*C*, *D*). As expected and hinted at theoretically (Wilson & Callaway, 2000), the large somatic compartments are slow pacemakers, but smaller dendritic compartments are fast pacemakers, so the final SFR should be determined from the sum of

all activities of these two compartments. The simulated results shown in Fig. 2 exactly match this case. But these simulation results based on the whole dendrites have not been tested in real DA neurons.

To examine whether the soma size of DA neurons influences SFRs similarly in real DA neurons, we measured SFRs in dissociated DA neurons having different soma sizes using a nystatin-perforated current-clamp

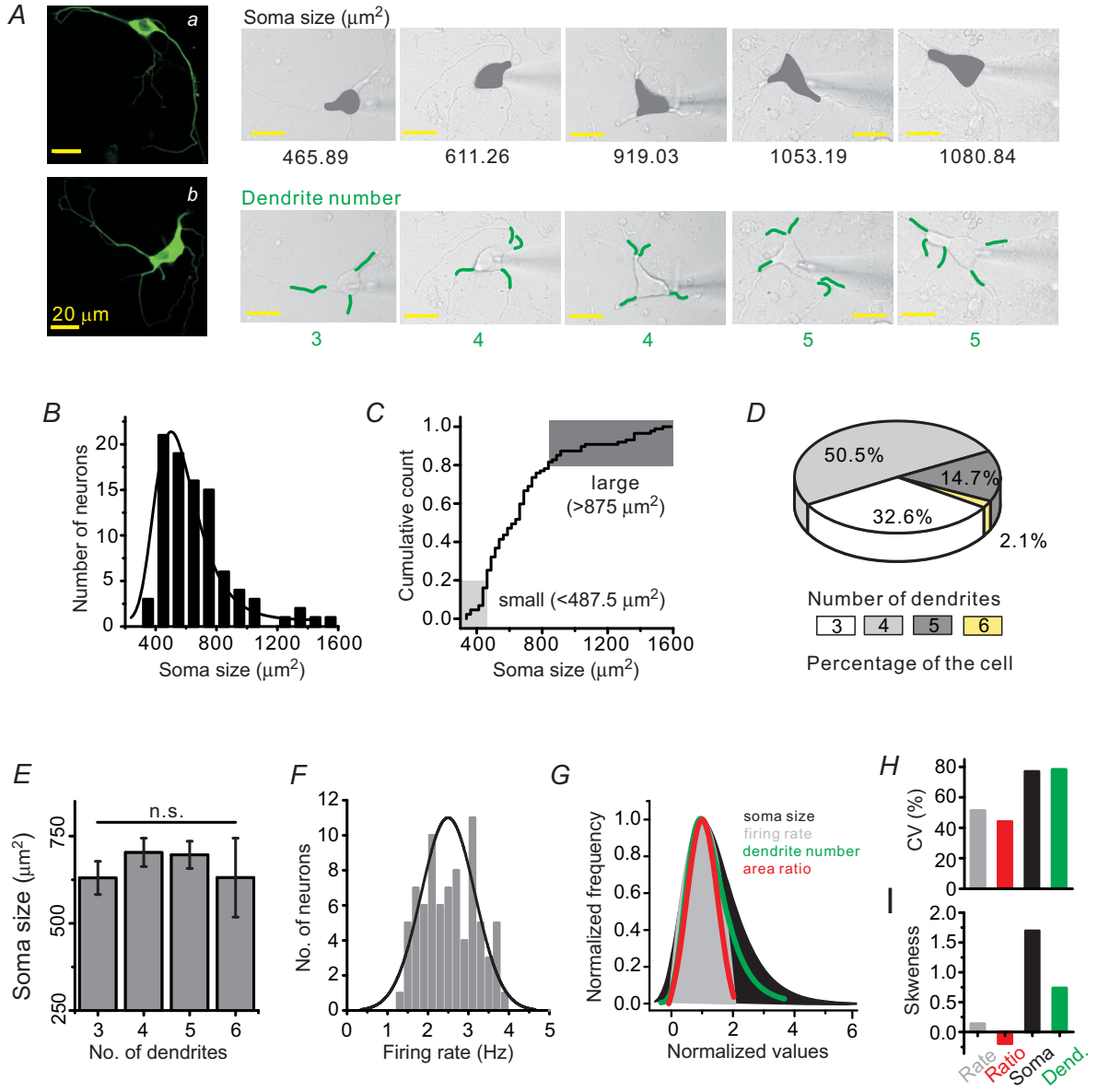

Figure 1. Morphological diversity of midbrain DA neurons
A, isolated midbrain neurons were identified as DA neurons by immunocytochemistry: fluorescence images of TH antibodypositive neurons (*a* and *b*). The diversity of soma size and dendrite numbers in the isolated DA neurons: DA neurons show different sizes of the soma (grey areas) and different numbers of dendrites (green lines). *B*, histogram and distribution curve of soma size in isolated DA neurons (bin size = 100 μm^2, n = 92). *C*, cumulative count of soma size. *D*, pie chart showing the percentage distribution of neurons. *E*, no correlation between the number of primary dendrites and soma size of DA neurons (n = 89). *F*, normal Gaussian distribution of SFR (n = 79). Bin size is 0.2 Hz in the histogram (minimum frequency = 1.2 Hz, maximum frequency = 3.8 Hz). *G*, comparison between the normalized distribution curves of soma size (black), SFR (grey), dendrite number (green) and proximal dendritic compartment/soma area ratio (red). *H*, SFR (51.2%) and the area ratio of proximal dendrites to the soma (44%) show less variability than do the distributions of soma size (76.8%) and numbers of dendrites (78.2%). *I*, skewness coefficient also differed with firing rate (0.14), area ratio (−0.19), soma size (1.7) and the number of dendrites (0.74).

patch-clamp recording. As shown in Fig. 3, a typical small neuron (Fig. 3*Aa*, soma size = 390.88 μm^2) and a large neuron (Fig. 3*Ab*, soma size = 1113.53 μm^2) fired at similar rates ($a = 2.03 \pm 0.11$ Hz and $b = 1.99 \pm 0.13$ Hz). That is, despite their more than twofold difference in calculated somatic areas, there is no apparent difference between them in firing rate. Figure 3*B* shows the results for the relationships between soma size and SFR in the 87 DA neurons recorded. As soma size increased, the SFRs did not significantly change in the DA neurons ($R^2 = -0.01$ in Fig. 3*B*, $n = 87$).

Other important morphological factors determining neuronal excitability could be the number of primary dendrites and the length of total dendrites. In the somatosensory cortex, interneurons in layer 2/3 showed a correlation between the electrical properties and the number of primary dendrites (Helmstaedter *et al.* 2009). Therefore, next, to examine the relationship between dendrite numbers and SFRs in the DA neurons, we examined the SFRs measured in the dissociated DA neurons that had different numbers of primary dendrites. As shown in Fig. 3*C*, one typical DA neuron (*a*, soma size = 465.89 μm^2) attached with three dendrites fired at 2.3 ± 0.02 Hz, and another DA neuron (*b*, soma size = 530.46 μm^2) with five primary dendrites fired at 2.31 ± 0.11 Hz (Fig. 3*C*), showing no apparent difference between neurons having similar soma sizes but different numbers of dendrites. When we plotted the SFRs with respect to the dendrite numbers in many dissociated DA neurons, the mean firing frequencies in the DA neurons with three, four, five and six dendrites were 2.46 ± 0.16 Hz ($n = 33$), 2.29 ± 0.11 Hz ($n = 48$), 2.5 ± 0.22 Hz ($n = 19$) and 2.3 ± 0.40 Hz ($n = 3$), respectively (Fig. 3*D*). There was no significant difference between them ($R^2 = -0.005$ in Fig. 3*D*). In a separate analysis, there was also no correlation between total lengths of dendrites and SFRs ($R^2 = -0.03$, $n = 31$, data not shown). This result is also different from expectations based on the simulation data (Fig. 2). From these results, we conclude that the SFR of real DA neurons cannot be determined by soma size or by dendrite numbers.

TTX puff and local Ca^{2+} perturbation experiments reveal importance of the proximal dendritic compartment in pacemaking activity in DA neurons

Usually, the axon initial segment is a site of AP generation that originates from the soma and requires high Na^+ channel density (Kole *et al.* 2008). However, in most DA neurons, the axon originates from the proximal dendrites and, interestingly, axon initiation sites mostly locate at the proximal dendritic site (30–70 μm from the soma) in DA neurons (Hausser *et al.* 1995; Gentet & Williams, 2007; Kole *et al.* 2008). In addition, it has been reported that both APs and Ca^{2+} spikes measured at dendrites

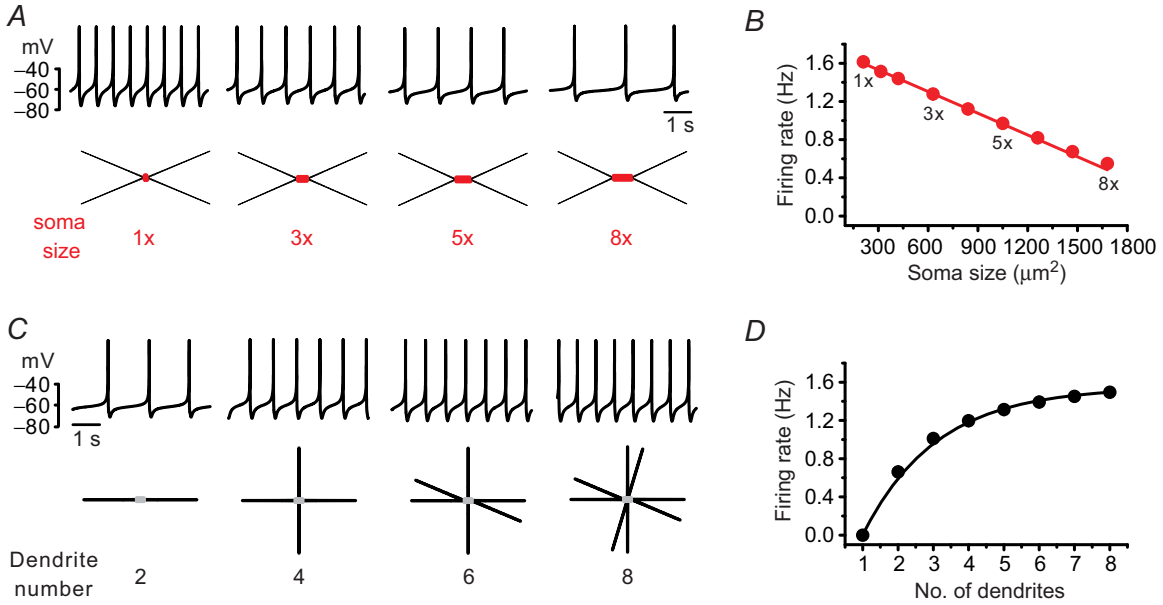

Figure 2. Relationship between soma size or number of dendrites and SFR in the model DA neurons
A, traces of the firing simulation (up) and schematic images of the model's DA neurons (bottom). The soma size of model neurons: 1× = 210 μm^2, 3× = 630 μm^2, 5× = 1050 μm^2 and 8× = 1680 μm^2. *B*, the relationship between soma sizes and the SFR in the model's DA neurons. There is a linear correlation between soma sizes and SFRs ($R^2 = 0.99$). *C*, traces of firing (up) and the schematic images of the model's DA neurons with different numbers of dendrites (bottom). *D*, the relationship between the number of primary dendrites and SFR in model neurons.

during pacemaking cycle are synchronized with those of the soma (Wilson & Callaway, 2000; Gentet & Williams, 2007). Therefore, it has been assumed that pacemaking activity in DA neurons can be determined by the electrical coupling between the soma and dendrites (Wilson & Callaway, 2000). This has led to the further assumption that the entire tapering dendrite is critically important for the generation of spontaneous firing and determination of firing rates in the DA neurons (Wilson & Callaway, 2000). However, the extent to which the dendritic compartments, such as proximal and distal dendritic compartments, participate in determining the SFR in real DA neurons has not been examined. Therefore, to examine what parts of dendrites play a key role in pacemaking, using a microinjection system we performed local TTX puff experiments along a dendrite to locally suppress Na^+ channels and pacemaker potential. Local applications of TTX (1 μM) inhibited the Na^+ channels and TTX-sensitive subthreshold sodium currents important for pacemaking (Puopolo *et al.* 2007) in the specific compartment applied, thereby suppressing or delaying generation of pacemaker potential at the application site. As shown in Fig. 4*A*, to avoid the unwanted spread of the applied TTX, an injection pipette was directed to the bath solution flow exit. When TTX was applied to the distal dendrites far from the soma, spontaneous firing was not affected significantly, but when the micropipette approached the proximal dendrites, the SFR began sharply decreasing around 80 μm from the soma (Fig. 4*A*–*C*). TTX puffs to the proximal dendritic compartments induced a strong reduction of SFR (control = 2.78 ± 0.24 Hz; TTX application = 0.92 ± 0.07 Hz, $n = 8$), whereas those to the distal dendritic region ≥80 μm from the soma did not change SFR significantly (2.44 ± 0.12 Hz, $n = 8$), suggesting that the proximal dendritic compartment is more important for generation of spontaneous firing than the distal dendrites in the DA neurons. To verify further that the proximal dendrites ≤80 μm from the soma are

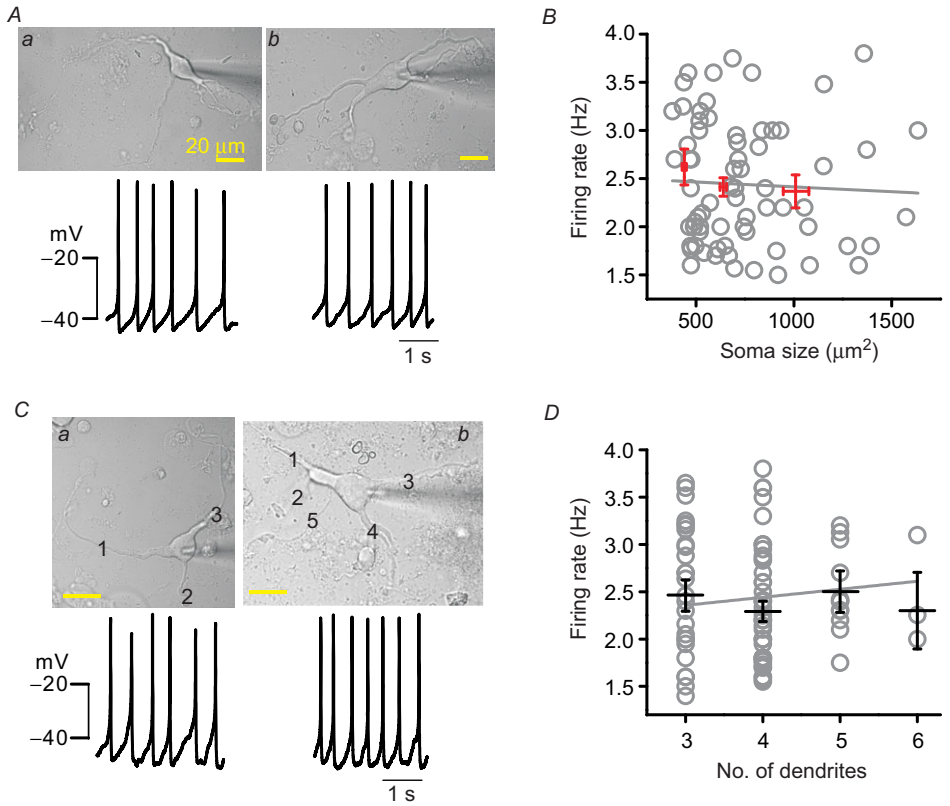

Figure 3. Soma size and the number of dendrites do not correlate with SFR in the isolated DA neurons
A, transmitted light images of DA neurons (up) and traces of spontaneous firing (bottom). *B*, the relationship between soma size and firing rates in the 87 isolated DA neurons. The red lines represent the mean firing rates and standard error in three groups of DA neurons: small soma (441 ± 10.84 μm^2 and 2.62 ± 0.19 Hz, $n = 16$), medium soma (639.13 ± 16.80 μm^2 and 2.41 ± 0.09 Hz, $n = 46$) and large soma (1009.22 ± 65.49 μm^2 and 2.37 ± 0.17 Hz, $n = 25$). There was no correlation between soma size and SFR ($n = 87$, $P > 0.05$). *C*, similar spontaneous firing rates in representative DA neurons having three dendrites (*a*) or five dendrites (*b*). *D*, the relationship between the number of primary dendrites and SFR in DA neurons. The black lines represent the mean firing rates with standard error (three dendrites: 2.46 ± 0.17, four dendrites: 2.29 ± 0.11, five dendrites: 2.50 ± 0.22, six dendrites: 2.30 ± 0.40, $n = 95$, $P > 0.5$).

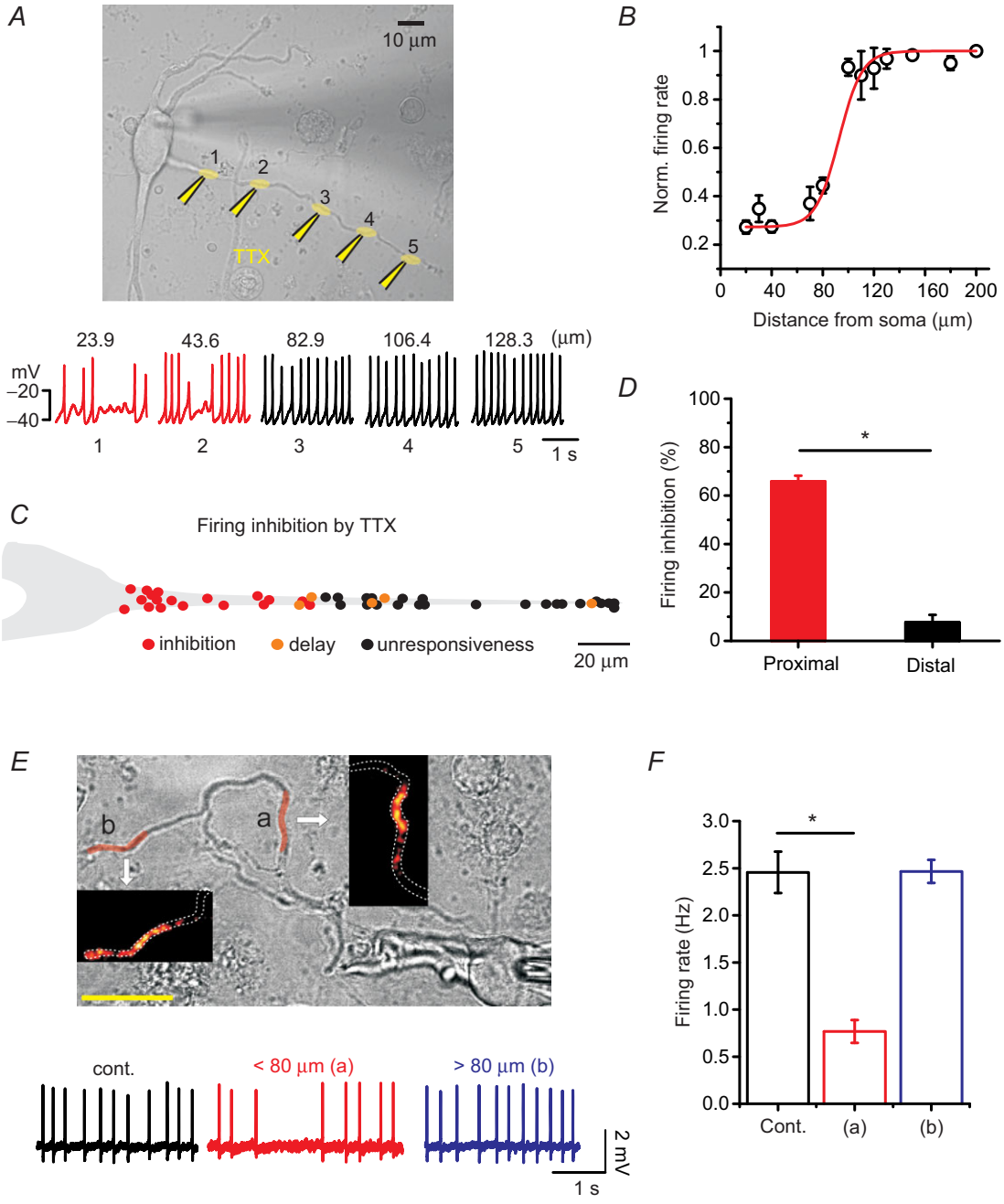

Figure 4. Importance of the proximal dendritic compartment for determining SFR in DA neurons
Spontaneous firing activity was perturbed by local application of TTX or Ca^{2+} uncaging in the isolated DA neurons. *A*, transmitted light image of a DA neuron and TTX puff sites (1 μM, yellow) and the recorded firing activities are shown at the time of TTX application at the marked site of a dendrite. *B*, the relationship between normalized firing rates and TTX puff locations along a dendrite (each point from 1–6 trials, $n = 8$). *C*, simplified SFR inhibition map along a dendrite. The red, orange and black circles indicate clear firing inhibitions (skip of more than one spontaneous firing or delay of spontaneous firing rate more than 50%), a delay of spontaneous firing rate by 10~50% and no inhibition, respectively. *D*, bar graph of the firing inhibitions by TTX puffs in the proximal and distal dendritic compartments ($n = 8$; $^*P = 1.12\times10^{-7}$, one-way ANOVA). *E*, Ca^{2+} uncaging induced highly localized Ca^{2+} rises within the uncaged dendritic area as shown in colour intensity graphs in the insets. Each uncaging area is marked by red on the dendrite of a transmitted DA neuron image. Firing traces are recorded at the control (black) and at the time of Ca^{2+} uncaging over the proximal (*a*, red, 59.8 μm from soma) and distal (*b*, blue, 112.4 μm from soma) dendritic compartments. *F*, bar graph of the SFR changes by Ca^{2+} uncaging in the proximal and distal dendritic compartments ($n = 4$; $^*P = 1.08\times10^{-4}$).

critical parts for determining pacemaker activity, next we tried to perform local Ca^{2+} perturbation experiments in which we raised $[Ca^{2+}]_i$ in a distal or proximal dendritic region separately using caged Ca^{2+} compounds and then observed SFR, as pacemaking cycles are easily affected by Ca^{2+} rises due to the high expression of small conductance calcium-activated potassium channels (SK channels) in this neuron (Wolfart & Roeper, 2002; Ji *et al.* 2009; Kim *et al.* 2013). As shown in Fig. 4*E*, in the 10 μM NP-EGTA loaded DA neurons we increased local Ca^{2+} concentration in the proximal or distal region of a dendrite and measured spontaneous firing activities. Areas marked in red are the uncaging areas and the consequential fluorescence images of local dendritic Ca^{2+} rises are presented in the insets. While Ca^{2+} rises in the proximal dendritic region strongly suppressed SFR (control = 2.46 ± 0.22 Hz; NP-EGTA uncaging = 0.77 ± 0.12 Hz, $n = 4$, $P = 1.08\times10^{-4}$, 'a' of Fig. 4*E*), Ca^{2+} rises in the distal dendritic region by uncaging similar areas did not affect the SFR (2.47 ± 0.12 Hz, $n = 4$, $P = 0.99$, 'b' of Fig. 4*E*), indicating the greater vulnerability of pacemaker activity to Ca^{2+} perturbation in the proximal dendrites than in the distal dendrites. These data also suggest that the proximal dendritic compartment is more important for generation of spontaneous firing than the distal dendrites in the DA neurons.

These results seem to be completely different from those of the theoretically proposed models of dopamine neurons in which major ion channels determining pacemaker activities are distributed homogenously throughout the entire dendrites (Wilson & Callaway, 2000; Medvedev *et al.* 2003). In these models, distal dendritic regions seem to participate significantly in pacemaker activities. To confirm this, we used the previously used simulation model (Fig. 2) in which the entire dendritic compartment possesses a similar excitability. As shown in Fig. 5, in this model we serially stimulated a neuron by using a local 'Iclamp' protocol at the soma (S), proximal dendritic compartment (P, 40 μm from soma), and two distal dendritic compartments, 1 and 2 (D1, 230 μm from the soma; D2, 380 μm from the soma), respectively (Fig. 5*A*). Step current injection to these sites led to two distinct responses in spontaneous firing: firing enhancement and the subsequent suppression of firings (Fig. 5) as described in acutely isolated real dopamine neurons (Kim *et al.* 2004). Enhancements of firing frequency between the S (7.95 ± 0.32 Hz), P (7.96 ± 0.32 Hz) and D1 site (7.51 ± 0.09 Hz) were similar (Fig. 5*B*), although current injection to the D2 site, a very long distance from the soma, was little different from other locations (5.85 ± 0.06 Hz, $p = 0.004$), indicating the substantial contribution to pacemaking of the distal dendrite far from the soma. Suppression responses were also similar (S = 0.87 Hz, P = 0.87 Hz, D1 = 0.73 Hz, D2 = 0.95 Hz, Fig. 5*B*). All these data suggest that the real DA neurons are not similar to the model DA neuron based on the homogenous properties of the entire dendrite. In model neurons distal dendrites seem to participate significantly in pacemaking, but the distal dendrites in real DA neurons appear to play a minimal role in pacemaking.

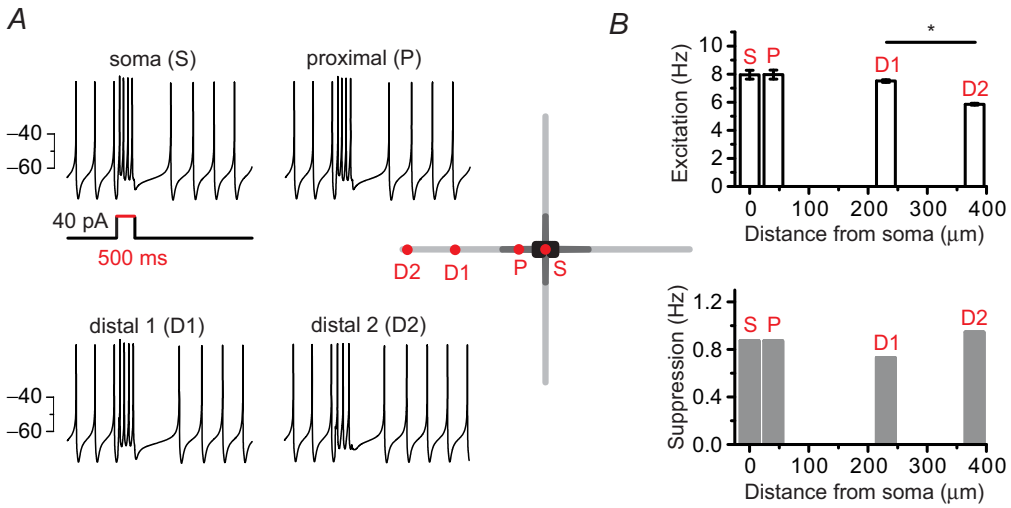

Figure 5. A model neuron based on the homogeneous properties of the entire dendrite shows substantial contribution of a distal dendrite to pacemaker activities
A, current injection to a various part of a model DA neuron affected spontaneous firing activities: firing enhancement during the current injection and post-stimulatory subsequent pause of firing. Schematic shape of a model neuron and each stimulation site are presented in the centre. The red spots of the model neuron showed current injected locations. A 40 pA current was injected for 500 ms. *B*, firing changes were classified into excitation during the stimulation and post-stimulatory inhibitions. Bar graphs represent the firing frequencies of excitation (upper) or inhibition (bottom) responses (*$P = 0.02$).

Local glutamate uncaging experiments show a higher excitability of the proximal dendritic compartment than distal dendritic compartments in DA neurons

To examine further the regional difference of excitability along a dendrite, we serially stimulated a small area of a dendrite with MNI-glutamate photolysis and then observed AP generation in the DA neurons (Fig. 6). To this end, a small amount of hyperpolarizing current (10–15 pA) was injected through the patch pipette to inhibit spontaneous firing activities (Fig. 6*A*, bottom panel). As the resting membrane potential was hyperpolarized from −46.46 ± 1.63 to −53.10 ± 1.49 mV ($n = 12$, Fig. 6*A*), the spontaneous firing was suppressed completely. In this condition, local glutamate uncaging with MNI-glutamate on a small area of a dendrite (Fig. 6*A*, circles) generated a tiny depolarization of membrane potential like an excitatory postsynaptic potential, with or without APs, according to the circumstances (Fig. 6*B*). As shown in Fig. 6*A* and *B*, local glutamate uncaging in the proximal dendritic area (denoted by circles 1, 6, 5 and 2 in Fig. 6*A*) evoked an AP, but failed in the distal dendrite (denoted by circles 3 and 4). When they failed, successive glutamate uncaging sometimes generated an AP in the borderline zone but did not in the remote area > 80 μm (Fig. 6*B*, lower traces). The local glutamate uncaging was performed according to the order of circle numbers (Fig. 6*A*). To evaluate the dendritic excitability along a dendrite, we plotted AP incidences after local glutamate uncaging several times as a function of distance from the soma (Fig. 6*C*). With the same stimulations (uncaging areas and durations), AP generation was dramatically decreased from the dendritic regions > 80 μm from the soma. Between these two zones AP incidences were dramatically different (Fig. 6*C* bottom, proximal dendritic compartment = 82.45 ± 7.66%, distal dendritic compartment = 12.5 ± 8.54%, $n = 12$). In Fig. 6*D* the AP incidences according to the uncaging

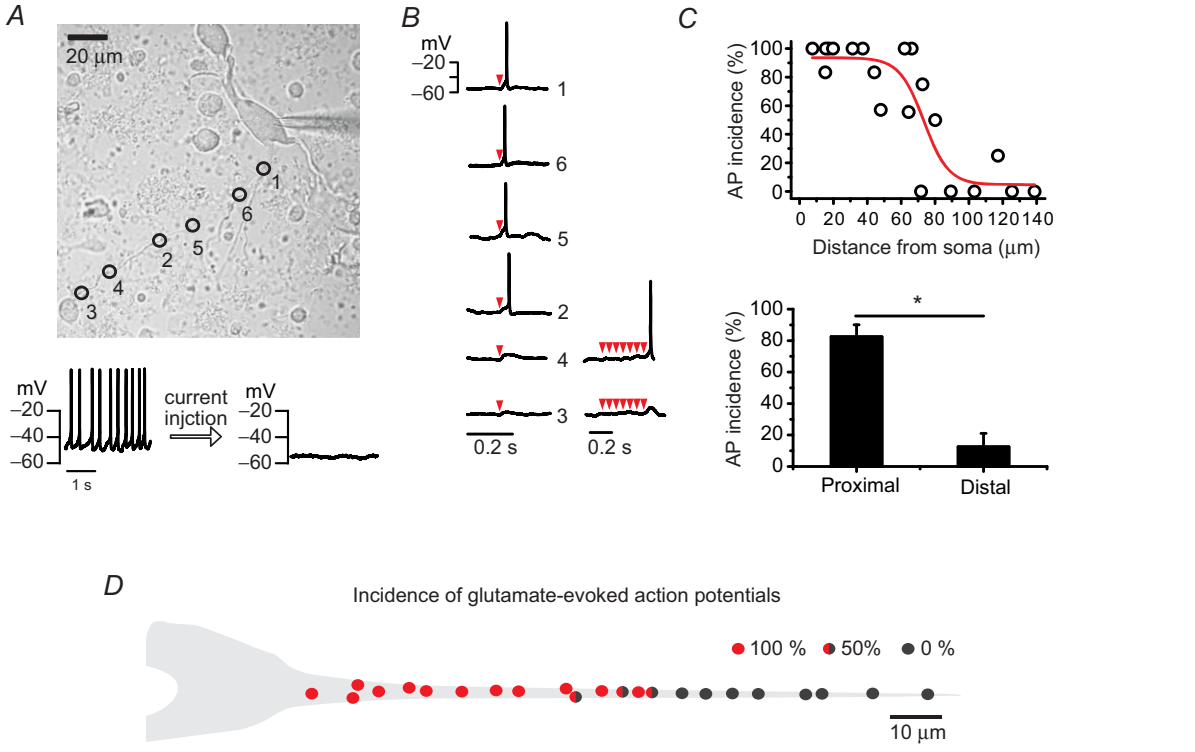

Figure 6. Different excitability between the proximal dendritic compartment and the distal compartment in DA neurons
AP was generated by localized glutamate uncaging under the silencing of DA neurons with hyperpolarizing currents. *A*, transmitted light image of a DA neuron marked with uncaging sites and orders (up). Spontaneous firing was suppressed by hyperpolarizing current (10–15 pA) injection. *B*, AP traces evoked by local MNI-caged glutamate uncaging. Red arrowheads indicate trials of uncaging. *C*, the relationship between the incidences of glutamate-evoked APs and stimulation locations along a dendrite (up). The proximal dendritic compartment shows higher AP incidence than the distal dendritic compartment ($n = 12$, $^*P = 4.27 \times 10^{-5}$). *D*, a simplified figure of AP incidence distributions along a dendrite. Incidence percentages are calculated from the number of AP generation successes/the number of total trials (4–6). The red or black closed circles indicate that all trials generated APs or failed to generate APs, respectively. The circles filled by red, black and half-and-half indicate 100, 0 and 50% incidence of APs, respectively.

locations are graphically presented with AP generation percentages (4–6 trials at each uncaging site, $n = 12$). Although an AP was always evoked in the proximal dendrite, it was difficult to evoke one in the distal dendrites > 80 μm (AP incidence; red = 100%, red and black = 50%, black = 0%, Fig. 6*D*). When we examined expression of *N*-methyl-D-aspartate (NMDA) and α-amino-3-hydroxy-5-methyl-4-isoxazolepropionic acid (AMPA) receptors (NR1 and GluR1) along a dendrite, there were no clear differences between them (data not shown). All these data indicate different dendritic excitability between the proximal dendrite and the distal dendrite in the DA neurons.

Therefore, we tried to plot the areas of the proximal dendrites ≤ 80 μm with respect to SFR, to examine whether the SFR is determined by the proximal dendritic compartments. However, the SFR of DA neurons did not directly correlate with the areas of the proximal dendrites ($R^2 = -0.01$ in Fig. 7*A*, $P = 0.63$ between the three groups in Fig. 7*C*). As neither the numbers nor the total lengths of dendrites correlated with SFR (Fig. 3*D*), and because soma size and dendrite number were highly variable (Fig. 1*A*, *H*), the SFR may not be reflected by the area of the proximal dendritic compartment. Consequently, the calculated areas of the proximal dendrites ≤ 80 μm were widely scattered regardless of dendrite numbers (Fig. 7*B*). From these results, we concluded that the excitable proximal dendritic compartment is important for generation of spontaneous firing activity, but the proximal dendritic compartment alone is not a determining factor for SFR.

Somatodendritic balance: the area ratio of the proximal dendritic compartment to the somatic compartment correlates with SFR

The variability of the morphological features (i.e. soma size and primary dendrite number) is higher than that of the SFRs in the DA neurons (Fig. 1*G*). Despite the morphological variations of DA neurons, the SFR seems to be maintained within a narrow range (Fig. 1*F*). How can this be explained?

Many papers including simulation studies suggest that the soma and the whole dendritic compartment are essential parts for generating and determining spontaneous firing activities in DA neurons (Kuznetsov *et al.* 2006; Tucker *et al.* 2012). According to the widely accepted coupled oscillator model (Wilson & Callaway, 2000; Medvedev *et al.* 2003), the SFR is determined by electrical coupling between the slow oscillating somatic compartment and the fast oscillating dendritic compartment. Thus, in their simulation model, the balance between the soma and the whole tapering dendritic compartment plays an important role in determining SFR. Thus, rather than including all the dendrites, we postulated that the soma and the proximal dendritic compartments together play an important role in determination of SFR in DA neurons. Therefore, we examined the relationship between area ratios of the proximal dendritic compartments (≤ 80 μm from the soma) to the soma compartment and the rate of spontaneous firing in the dissociated DA neurons. As the dissociated DA neurons have variously sized somata as well as differing numbers of primary dendrites, we measured the soma sizes and areas of proximal dendritic compartments in every DA neuron. We then sorted and rearranged them according to the area ratio of the proximal dendritic compartment to the soma (Fig. 8*A*). The grey colour map represents normalized values of the proximal dendritic areas, the soma areas and the area ratio between them in the 37 recorded DA neurons (Fig. 8*A*). For comparison, we categorized all analysed DA neurons into four groups (Fig. 8*A*, *B*). The soma and proximal dendritic compartments were divided into small (lower 20%) and large areas (upper 20%) by the size distribution curves.

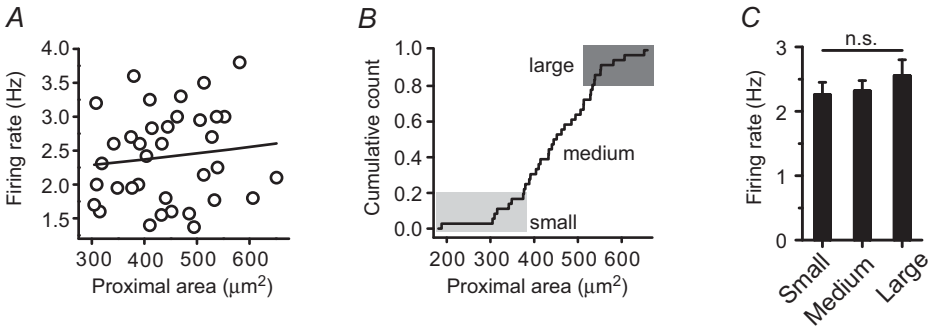

Figure 7. Relationship between the proximal dendritic compartment and SFR in DA neurons
A, no correlation between proximal dendritic areas and SFRs in the isolated DA neurons ($n = 36$, $R^2 = -0.01$). *B*, cumulative count of proximal dendritic areas. *C*, no correlation between the size of proximal dendritic compartments and SFR (small proximal area: 327.70 ± 8.79 μm^2 with frequency of 2.26 ± 0.19 Hz, medium proximal area: 447.76 ± 10.89 μm^2 with frequency of with 2.32 ± 0.16 Hz, large proximal area: 569.05 ± 14.67 μm^2 with frequency of with 2.55 ± 0.25 Hz, $n = 36$, $P = 0.63$). n.s., No significant difference.

The large proximal dendritic area was over 533.1 μm^2, and the small area was <376.5 μm^2 (Fig. 7*B*). Therefore, the isolated neurons can be classified into four groups: large proximal dendrites with a large soma (L/L, dark grey), small proximal dendrites with a large soma (S/L, blue), large proximal dendrites with a small soma (L/S, red) and small proximal dendrites with a small soma (S/S, light grey, Fig. 8*B*, left). The populations of L/S, L/L, S/S and S/L neurons were 18.9% (7/37), 8.1% (3/37), 8.1% (3/37) and 16.2% (6/37), respectively. If our assumption is correct, each group of neurons having different area ratios will have a different SFR (Fig. 8*B*, right), theoretically. When we plotted the SFRs against the proximal dendritic compartment/soma area ratio, we found that SFR was strongly correlated with the area ratio in the dissociated DA neurons; the higher the area ratio, the higher the SFR (R^2 of blue and red circles = 0.67, Fig. 7*C*). The slowest frequencies of spontaneous firing (1.91 ± 0.13 Hz) were recorded in the neuron group having the smallest area ratios (0.36 ± 0.05 ratio, S/L group, closed blue circles in Fig. 8*C*). But, the neurons that had the highest area ratios (L/S group, closed red circles in Fig. 8*C*) showed the fastest firing frequencies (2.81 ± 0.15 Hz, 1.05 ± 0.03 ratio). The other groups of DA neurons, which have large proximal dendrites with a large soma or small proximal dendrites with a small soma, showed frequencies of 2.1 ± 0.29 and 2.11 ± 0.26 Hz (Fig. 8*C*, *E*), respectively. Figure 8*D* shows the typical DA neurons of large (*a*) and small (*b*) proximal compartments/soma area ratios and corresponding spontaneous firing traces. The L/S neuron (Fig. 8*Da*) with a small soma (358.64 μm^2) and a large proximal dendritic compartment (344.29 μm^2)

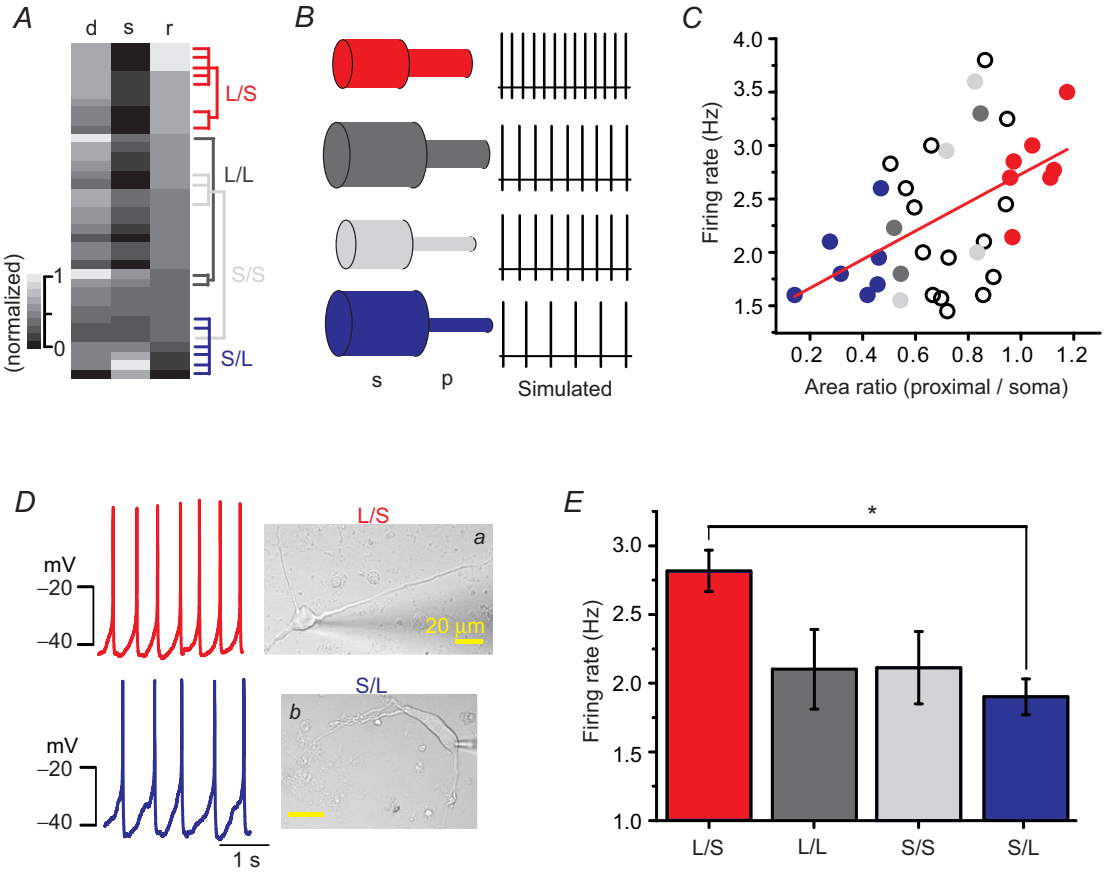

Figure 8. The ratios of proximal dendritic area to soma area determine intrinsic excitability of DA neurons

A, heat map graph showing the wide variety of areas of the proximal dendrites, soma sizes and the area ratio of proximal dendrites to soma. All values are normalized. Neurons were allocated to four groups. *B*, simplified neuron models and simulated spontaneous firing of each model. Model neurons are classified according to soma size and the area of proximal dendrites. *C*, SFR increases with the area ratio of the proximal dendrites to the soma. The red closed circles indicate a neuron that has a large proximal dendritic area and small soma, and the blue closed circles indicate a neuron that has a low area ratio of small proximal compartments to large soma ($n = 37$). *D*, transmitted light images of representative types of neurons in different groups and corresponding firing traces: *a*, large proximal dendrites and small soma (L/S); *b*, small proximal dendrites and large soma (S/L). *E*, comparison of SFRs in different groups of DA neurons ($n = 37$, $^*P = 0.04$).

showed an area ratio of 0.96 and a firing rate of 2.67 ± 0.13 Hz, whereas the S/L neuron (Fig. 8*Db*) with a large soma (1331.58 μm^2) and a small proximal dendritic compartment (186.42 μm^2) showed a 0.14 area ratio and a 1.6 ± 0.22 Hz SFR. These results suggest that the area ratio of the proximal dendritic compartments to the soma compartment can determine the SFR in DA neurons. Mean values of SFRs in different groups are summarized in Fig. 8*E*. Interestingly, the distribution curve of the proximal dendritic compartments/soma area ratio is very similar to the Gaussian curve of the SFR (Fig. 1*G*).

Discussion

Spontaneously firing DA neurons exhibit dendritic excitability, and an axon mostly originates from a proximal dendritic site (Grace & Bunney, 1984*a*,*b*; Tepper *et al.* 1987; Hausser *et al.* 1995; Blythe *et al.* 2009), and if there are no external afferent inputs, they show regular spontaneous APs at 2–5 Hz (Grace & Onn, 1989; Hainsworth *et al.* 1991; Choi *et al.* 2006; Kim *et al.* 2007). Treatment with TTX abolishes APs completely, but slow oscillatory potentials (SOPs) survive at slower and/or similar frequencies to the original pacemaking frequencies (Grace, 1991; Amini *et al.* 1999; Chan *et al.* 2007; Gentet & Williams, 2007; Guzman *et al.* 2009). SOPs appear to be mirrored by oscillations of $[Ca^{2+}]_i$ in which voltage-operated Ca^{2+} channels (VOCCs), including $Ca_v1.3$ channels and SK channels, seem to open and close alternately (Wilson & Callaway, 2000; Chan *et al.* 2007). As the rates of $[Ca^{2+}]_i$ rise and removal depend on the size of the compartment (i.e. a large soma or a small part of a dendrite, due to differences in the surface area/volume ratio), the coupled oscillatory model (Wilson & Callaway, 2000) has been proposed and widely accepted (Surmeier *et al.* 2012); in that way, the SFR could be determined by the electrical coupling between the slow oscillating soma compartment and the fast oscillating dendritic compartment (Wilson & Callaway, 2000; Kuznetsova *et al.* 2010; Drion *et al.* 2011; Tucker *et al.* 2012). The simulation experiments shown in Fig. 2 represent this case; the SFR is correlated with the number of dendrites, but inversely correlated with soma size. It has therefore been assumed that the SFR is determined by the contribution of the entirety of the membrane compartments (see the coupled oscillator model; Wilson & Callaway, 2000), without clear experimental evidence. Currently, despite its fundamental importance, little is known about the morphological features of the real DA neurons that govern the SFR. This may be partly due to the difficulties in analysing morphologies of DA neurons in the midbrain tissue together with firing measurements, in which multiple dendrites do not extend in a simple direction and the shape of somata is highly variable (Fig. 1*A*). Another difficulty arises from the vulnerability and complexity of the SFR, which is easily affected by many neurohormones and neurotransmitters and nearby network activities seen in brain slices (Meltzer *et al.* 1997; Kitai *et al.* 1999; Morikawa & Paladini, 2011). Therefore, by taking advantage of acutely isolated SNc DA neurons that preserved a substantial amount of dendrites and regular spontaneous firing activities, we have now pursued identification of the morphological features that determine the SFR in detail. In this condition, pure intrinsic excitability reflected by the SFR can be more correctly measured without any complex interactions with neighbouring cells and environmental hormones and factors, and so morphologies can be easily analysed (Fig. 1; see also Choi *et al.* 2003; Kim *et al.* 2007; Jang *et al.* 2011*a*). Benefits and functional similarity of dissociated DA neurons to those in midbrain slices have been demonstrated in other groups (Hahn *et al.* 2003; Puopolo *et al.* 2007).

In principle, morphology determines function and vice versa (Lee & Van Vactor, 2003); thus, the morphological properties of a neuron can determine intrinsic excitability, and therefore could be reflected in either the size of the soma or the dendritic topology (Fig. 2). Isolated DA neurons from the rat SNc showed a wide range of soma size and variable numbers of primary dendrites (Fig. 1*A*–*D*) but preserved a quite consistent SFR (Fig. 1*F*). This may indicate that individual midbrain DA neurons bearing coupled, multiple, excitable compartments should have a tuning mechanism to maintain optimum ranges of SFR, which will be achieved via a harmonized balance between excitable compartments. To investigate this hypothesis, we had first tried to identify unequal distributions of some ion channels (data not shown), including Na_v channels, which appear to have active roles in pacemaking (Khaliq & Bean, 2010; Tucker *et al.* 2012). But unfortunately, we did not detect any significant localization of ion channels with immunocytochemical staining. This does not mean that pacemaking channels are ubiquitously distributed throughout the whole somatodendritic compartment, but rather indicates that the direct demonstration of localization of ion channels involved in pacemaking is difficult with these tools. In this regard, Tucker *et al.* (2012), using dynamic clamping techniques, suggested that Na_v channels seem to be differently distributed in the somatodendritic tree, which could be critical for determination of excitability.

Therefore, we performed correlation studies between morphologies and SFRs in DA neurons, and we showed that neither soma size nor the number of primary dendrites was correlated with SFR (Fig. 3) but that SFR was strongly correlated with the area ratios of the proximal dendritic compartments to the somatic compartment (Fig. 8). To reach the conclusion that the excitability of the proximal dendritic compartment is different from that of the distal part of dendrites, we employed a micro-pressurized injection system with which we could locally

apply TTX to a distal or proximal dendritic region and Ca^{2+} perturbation experiments (Figs 4 and 5). Elimination of excitability from the distal dendrites by TTX puff had no effect on SFR, but suppression of the proximal dendritic region decreased SFR significantly (Fig. 4). Perturbation of Ca^{2+} signals in the distal dendrites had no effect on SFR but the same perturbation in the proximal dendrites strongly affected SFR (Fig. 4), which differ substantially from those in the simulation model based on the homogenous properties of the entire dendritic compartment (Fig. 5). In addition, we directly checked excitability of a dendrite by using glutamate uncaging experiments in which we could locally stimulate a part of a dendrite with glutamate and detect evoked APs. As shown in Fig. 6, the proximal dendritic compartment at ≤ 80 μm is highly excitable compared with the distal dendritic region, consistent with the results obtained via local TTX application and caged Ca^{2+} uncaging experiments (Fig. 4). Of course, glutamate receptors and signals are not equally distributed throughout the soma and dendrites in DA neurons (Jang *et al.* 2011*a*), but nevertheless glutamate signalling does not appear to have a clear-cut boundary between proximal and distal dendrites (Jang *et al.* 2011*b*). Therefore, it is more likely that endogenous excitabilities of the proximal dendritic region at ≤ 80 μm could be different from that of distal dendrites. Finally, as shown in Fig. 8, by arranging DA neuron shapes into the area ratio of the proximal dendritic region to the soma, we concluded that the SFR in the DA neuron can be determined by the electrical coupling between the soma and the proximal dendritic compartment, rather than the entire dendritic compartments. The consistency of the SFR, despite the morphological diversity of individual DA neurons, could be obtained by dynamic compartmental adjustments between the soma and the excitable proximal dendritic compartments in the DA neurons. All these data provide hints for future study about how pacemaking in DA neurons is functionally and geometrically organized.

References

Amini B, Clark JW Jr & Canavier CC (1999). Calcium dynamics underlying pacemaker-like and burst firing oscillations in midbrain dopaminergic neurons: a computational study. *J Neurophysiol* **82**, 2249–2261.

Ball J (2001). Current advances in Parkinson's disease. *Trends Neurosci* **24**, 367–369.

Blythe SN, Wokosin D, Atherton JF & Bevan MD (2009). Cellular mechanisms underlying burst firing in substantia nigra dopamine neurons. *J Neurosci* **29**, 15531–15541.

Chan CS, Guzman JN, Ilijic E, Mercer JN, Rick C, Tkatch T, Meredith GE & Surmeier DJ (2007). 'Rejuvenation' protects neurons in mouse models of Parkinson's disease. *Nature* **447**, 1081–1086.

Choi YM, Kim SH, Chung S, Uhm DY & Park MK (2006). Regional interaction of endoplasmic reticulum Ca^{2+} signals between soma and dendrites through rapid luminal Ca^{2+} diffusion. *J Neurosci* **26**, 12127–12136.

Choi YM, Kim SH, Uhm DY & Park MK (2003). Glutamate-mediated $[Ca^{2+}]_c$ dynamics in spontaneously firing dopamine neurons of the rat substantia nigra pars compacta. *J Cell Sci* **116**, 2665–2675.

Drion G, Massotte L, Sepulchre R & Seutin V (2011). How modelling can reconcile apparently discrepant experimental results: the case of pacemaking in dopaminergic neurons. *PLoS Comput Biol* **7**, e1002050.

Gentet LJ & Williams SR (2007). Dopamine gates action potential backpropagation in midbrain dopaminergic neurons. *J Neurosci* **27**, 1892–1901.

Grace AA (1991). Regulation of spontaneous activity and oscillatory spike firing in rat midbrain dopamine neurons recorded *in vitro*. *Synapse* **7**, 221–234.

Grace AA & Bunney BS (1983*a*). Intracellular and extracellular electophysiology of nigral dopaminergic neurons – 1. Identification and characterization. *Neuroscience* **10**, 301–315.

Grace AA & Bunney BS (1983*b*). Intracellular and extracellular electrophysiology of nigral dopaminergic neuorns – 2. Action potential generating mechanisms and morphological correlates. *Neuroscience* **10**, 317–331.

Grace AA & Bunney BS (1984*a*). The control of firing pattern in nigral dopamine neurons: single spike firing. *J Neurosci* **4**, 2866–2876.

Grace AA & Bunney BS (1984*b*). The control of firing pattern in nigral dopamine neurons: burst firing. *J Neurosci* **4**, 2877–2890.

Grace AA & Onn SP (1989). Morphology and electrophysiological properties of immunocytochemically identified rat dopamine neurons recorded *in vitro*. *J Neurosci* **9**, 3463–3481.

Guzman JN, Sanchez-Padilla J, Chan CS & Surmeier DJ (2009). Robust pacemaking in substantia nigra dopaminergic neurons. *J Neurosci* **29**, 11011–11019.

Guzman JN, Sanchez-Padilla J, Wokosin D, Kondapalli J, Ilijic E, Schumacker PT & Surmeier DJ (2010). Oxidant stress evoked by pacemaking in dopaminergic neurons is attenuated by DJ-1. *Nature* **468**, 696–700.

Hahn J, Tse TE & Levitan ES (2003). Long-term K^+ channel-mediated dampening of dopamine neuron excitability by the antipsychotic drug haloperidol. *J Neurosci* **23**, 10859–10866.

Hainsworth AH, Röper J, Kapoor R & Ashcroft FM (1991). Identification and electrophysiology from isolated pars compacta neurons from guinea-pig substantia nigra. *Neuroscience* **43**, 81–93.

Hausser M, Stuart G, Racca C & Sakmann B (1995). Axonal initiation and active dendritic propagation of action potentials in substantia nigra neurons. *Neuron* **15**, 637–647.

Helmstaedter M, Sakmann B & Feldmeyer D (2009). The relation between dendritic geometry, electrical excitability, and axonal projections of L2/3 interneurons in rat barrel cortex. *Cereb Cortex* **19**, 938–950.

Henneman E (1957). Relation between size of neurons and their susceptibility to discharge. *Science* **126**, 1345–1347.

Jang JY, Jang M, Kim SH, Um KB, Kang YK, Kim HJ, Chung S & Park MK (2011*a*). Regulation of dopaminergic neuron firing by heterogeneous dopamine autoreceptors in the substantia nigra pars compacta. *J Neurochem* **116**, 966–974.

Jang M, Jang JY, Kim SH, Uhm KB, Kang YK, Kim HJ, Chung S & Park MK (2011*b*). Functional organization of dendritic Ca^{2+} signals in midbrain dopamine neurons. *Cell Calcium* **50**, 370–380.

Ji H, Hougaard C, Herrik KF, Strøbaek D, Christophersen P & Shepard PD (2009). Tuning the excitability of midbrain dopamine neurons by modulating the Ca^{2+} sensitivity of SK channels. *Eur J Neurosci* **29**, 1883–1895.

Khaliq ZM & Bean BP (2010). Pacemaking in dopaminergic ventral tegmental area neurons: depolarizing drive from background and voltage-dependent sodium conductances. *J Neurosci* **30**, 7401–7413.

Kim SH, Choi YM, Chung S, Uhm DY & Park MK (2004). Two different Ca^{2+}-dependent inhibitory mechanisms of spontaneous firing by glutamate in dopamine neurons. *J Neurochem* **91**, 983–995.

Kim SH, Choi YM, Jang JY, Chung S, Kang YK & Park MK (2007). Nonselective cation channels are essential for maintaining intracellular Ca^{2+} levels and spontaneous firing activity in the midbrain dopamine neurons. *Pflugers Arch* **455**, 309–321.

Kim SH, Jang JY, Jang M, Uhm KB, Chung S, Kim HJ & Park MK (2013). Homeostatic regulation mechanism of spontaneous firing determines glutamate responsiveness in the midbrain dopamine neurons. *Cell Calcium* **54**, 295–306.

Kita T, Kita H & Kitai ST (1986). Electrical membrane properties of rat substantia nigra compacta neurons in an *in vitro* slice preparation. *Brain Res* **372**, 21–30.

Kitai ST, Shepard PD, Callaway JC & Scroggs R (1999). Afferent modulation of dopamine neuron firing patterns. *Curr Opin Neurobiol* **9**, 690–697.

Kole MH, Ilschner SU, Kampa BM, Williams SR, Ruben PC & Stuart GJ (2008). Action potential generation requires a high sodium channel density in the axon initial segment. *Nat Neurosci* **11**, 178–186.

Kuznetsov AS, Kopell NJ & Wilson CJ (2006). Transient high-frequency firing in a coupled-oscillator model of the mesencephalic dopaminergic neuron. *J Neurophysiol* **95**, 932–947.

Kuznetsova AY, Huertas MA, Kuznetsov AS, Paladini CA & Canavier CC (2010). Regulation of firing frequency in a computational model of a midbrain dopaminergic neuron. *J Comput Neurosci* **28**, 389–403.

Lee H & Van Vactor D (2003). Neurons take shape. *Curr Biol* **13**, R152–161.

Medvedev GS, Wilson CJ, Callaway JC & Kopell N (2003). Dendritic synchrony and transient dynamics in a coupled oscillator model of the dopaminergic neuron. *J Comput Neurosci* **15**, 53–69.

Meltzer LT, Christoffersen CL & Serpa KA (1997). Modulation of dopamine neuronal activity by glutamate receptor subtypes. *Neurosci Behav Rev* **21**, 511–518.

Mercuri NB, Bonci A, Calabresi P, Stratta F, Stefani A & Bernardi G (1994). Effects of dihydropyridine calcium antagonists on rat midbrain dopaminergic neurones. *Br J Pharmacol* **113**, 831–838.

Morikawa H & Paladini CA (2011). Dynamic regulation of midbrain dopamine neuron activity: intrinsic, synaptic, and plasticity mechanisms. *Neuroscience* **198**, 95–111.

Nedergaard S & Greenfield SA (1992). Sub-populations of pars compacta neurons in the substantia nigra: the significance of qualitatively and quantitatively distinct conductances. *Neuroscience* **48**, 423–437.

Puopolo M, Raviola E & Bean BP (2007). Roles of subthreshold calcium current and sodium current in spontaneous firing of mouse midbrain dopamine neurons. *J Neurosci* **27**, 645–656.

Putzier I, Kullmann PH, Horn JP & Levitan ES (2009). $Ca_v1.3$ channel voltage dependence, not Ca^{2+} selectivity, drives pacemaker activity and amplifies bursts in nigral dopamine neurons. *J Neurosci* **29**, 15414–15419.

Saywell SA, Ford TW, Meehan CF, Todd AJ & Kirkwood PA (2011). Electrophysiological and morphological characterization of propriospinal interneurons in the thoracic spinal cord. *J Neurophysiol* **105**, 806–826.

Stuart G, Racca C & Sakmann B (1995). Axonal initiation and active dendritic propagation of action potentials in substantia nigra neurons. *Neuron* **15**, 637–647.

Surmeier DJ, Guzman JN, Sanchez J & Schumacker PT (2012). Physiological phenotype and vulnerability in Parkinson's disease. *Cold Spring Harb Perspect Med* **2**, a009290.

Tepper JM, Sawyer SF & Groves PM (1987). Electrophysiologically identified nigral dopaminergic neurons intracellularly labelled with HRP: light-microscopic analysis. *J Neurosci* **7**, 2794–2806.

Tucker KR, Huertas MA, Horn JP, Canavier CC & Levitan ES (2012). Pacemaker rate and depolarization block in nigral dopamine neurons: a somatic sodium channel balancing act. *J Neurosci* **32**, 14519–14531.

Wilson CJ & Callaway JC (2000). Coupled oscillator model of the dopaminergic neuron of the substantia nigra. *J Neurophysiol* **83**, 3084–3100.

Wolfart J & Roeper J (2002). Selective coupling of T-type calcium channels to SK potassium channels prevents intrinsic bursting in dopaminergic midbrain neurons. *J Neurosci* **22**, 3404–3413.

Additional Information

Competing interests

The authors declare that they have no competing interests.

Author contributions

J.Y.J., H.J.K. and M.K.P. participated in conception and experimental design, and J.Y.J., K.B.U., S.H.K. and M.J. carried out the whole electrical and calcium experiments. K.B.U. performed computer simulation experiments. J.Y.J., M.J., K.B.U. and S.H.K. participated in the preparation of neurons and some electrophysiological studies. H.C., S.C. and H.J.K. helped with analysis of data, preparation of figures and the manuscript. J.Y.J. and M.K.P. drafted and revised the manuscript. All authors read and approved the final submission.

Funding

This work (NRF-2011-0029293) was supported by the Mid-career Researcher Program through an NRF grant funded by the MEST.

Acknowledgements

None declared.

Translational Perspective

In neurons, morphological properties are one of the major factors determining intrinsic excitabilities, which could therefore often be reflected either by the size of the soma, such as 'the size principle' in motor neurons, or by the dendritic topologies in some neurons. Individual midbrain dopamine neurons bearing multiple excitable dendrites *ex vivo* generate spontaneous and regular action potentials, showing intrinsic excitability. However, little is known about the geometrical factors determining intrinsic excitability in the midbrain dopamine neurons. Isolated dopamine neurons from the rat substantia nigra pars compacta showed a wide range of soma size and variable numbers of primary dendrites, but preserved a reasonably consistent spontaneous firing rate (SFR). Morphological analysis reveals that the SFR could be best correlated by the area ratio of proximal dendritic compartments to the somatic compartment, not by soma size or the number of primary dendrites. Elimination or perturbation of excitability from the distal dendrites by local tetrodotoxin puffs or by local Ca^{2+} uncaging had no effect on SFR, suggesting less importance of the distal dendrites in intrinsic excitability. All these data indicate that intrinsic excitability could be determined by the harmonic electrical balance between the soma and the proximal dendritic compartments. Therefore, like 'the size principle' in motor neurons, we propose 'the ratio principle' in that the area ratios of proximal dendritic compartments to the somatic compartment can determine excitability in midbrain dopamine neurons.